

Adaptive Orbital Direct-to-Device: Rethinking Satellite IoT Architectures

Hannaneh B. Pasandi¹, Mohammad Hosseini², Sina Dorabi³, Juan A. Fraire⁴, Franck Rousseau⁵

¹UC Berkeley, ²Shahid Beheshti University, ³USI Lugano, ⁴INRIA-Lyon, ⁵Univ. Grenoble Alpes
{h.pasandi@berkeley.edu, m.hosseini@sbu.ac.ir, sina.dorabi@usi.ch,
juan.fraire@inria.fr, franck.rousseau@imag.fr}

ABSTRACT

Current satellite Direct-to-Device (D2D) architectures often hard-commit to an orbital regime, forcing suboptimal trade-offs between latency, reliability, and energy. We present, to our knowledge, the first adaptive orbital D2D architecture that dynamically switches among LEO, GEO, and hybrid paths based on real-time Doppler, load, and application QoS. Validated via a LoRa satellite-IoT implementation, our approach improves capacity $3\times$ (936 vs. 312 nodes per gateway at 95% PDR), reduces tail latency by 62% (95th percentile: 342ms vs. 892ms), and lowers energy consumption by 31% via retransmission avoidance. Treating orbital choice as a dynamic optimization addresses core limitations of static designs and generalizes beyond LoRa to cellular and NB-IoT D2D systems, charting a path toward resilient, efficient space-terrestrial IoT. Our simulation is available online at [Adaptive Orbital Direct-to-Device](#).

1 INTRODUCTION

The explosive growth of Internet of Things (IoT) deployments—projected to reach 75 billion devices by 2030 [17]—has created an urgent need for ubiquitous connectivity beyond terrestrial infrastructure reach. Direct-to-Device (D2D) satellite communication emerges as a critical solution, offering low-power, long-range connectivity for the 2.7 billion users currently unconnected by terrestrial networks [7]. Recent commercial deployments validate this trend. SpaceX’s Starlink Direct-to-Cell partnerships with T-Mobile [16] demonstrate LEO satellite cellular connectivity. Apple’s Emergency SOS via Globalstar [1] enables satellite messaging for consumer devices. AST SpaceMobile’s cellular connectivity demonstrations [15] signal a paradigm shift toward satellite-enabled ubiquitous IoT connectivity.

However, current satellite D2D architectures suffer from a fundamental limitation: static orbital commitments. Existing deployments force a binary architectural choice between Low Earth Orbit (LEO) satellites offering low latency but suffering from coverage gaps and Doppler-induced failures, or Geostationary Earth Orbit (GEO) satellites providing reliable coverage but imposing energy penalties unsuitable

for battery-powered IoT devices. This static approach ignores the heterogeneous and dynamic nature of IoT workloads. Emergency alerts require sub-second to few-second latency targets (aligned with our <30 s delay-sensitive class), while environmental sensors tolerate hundreds of seconds (e.g., ≈ 300 s) of delay. Dense urban deployments (1000+ nodes/km²) have different optimization needs than sparse rural sensors. Traffic patterns vary from periodic sensor reports to bursty emergency communications, each benefiting from different orbital characteristics.

We present, to our knowledge, the first adaptive orbital D2D architecture that dynamically selects optimal transmission paths—LEO direct, GEO indirect, or hybrid operation—based on real-time Doppler conditions, gateway load, interference levels, and application QoS requirements. Our key insight is that treating orbital selection as a dynamic optimization problem, rather than a static deployment choice, unlocks significant performance gains previously thought impossible.

Contributions.

- Quantify static-architecture limits using TLE-derived Doppler feasibility and Iridium RF measurements.
- Design an adaptive orbital switching framework with MCU-class decision latency (sub-10ms in our simulated implementation).
- Demonstrate gains in simulation validated by real traces: $3\times$ capacity, 62% tail-latency reduction, 31% energy savings.
- Show generality to cellular/NB-IoT D2D beyond LoRa via an architecture-level formulation.

Limitations. Our current evaluation is simulation-heavy (validated against 847 real packets from FossaSat-2); large-scale field trials and multi-operator experiments are future work.

2 BACKGROUND AND MOTIVATION

2.1 D2D Satellite Architecture Taxonomy

Modern satellite D2D systems can be categorized along two dimensions—orbital regime and adaptation capability—as summarized in Table 1.

Orbital regime. LEO satellites (340–2000 km altitude) offer 20–50 ms latency but incur Doppler shifts up to ± 21.7 kHz, exceeding LoRa’s 7.6 Hz tolerance at 868 MHz by $\sim 2,700\times$ [5]; GEO satellites (35,786 km) provide stable 250–300 ms latency but require significantly higher link budgets (typically 15–20 dB more [2]), which can be prohibitive for energy-constrained IoT devices.

Adaptation capability. Current architectures fall into three categories—*static LEO-only* (e.g., Swarm Technologies [18] and Lacuna Space [14]) that commit to LEO despite Doppler and coverage gaps; *static GEO-only* (e.g., Thuraya [19] and Inmarsat) that provide reliable GEO connectivity at the cost of higher-power terminals; and *static hybrid* deployments that incorporate both LEO and GEO but rely on fixed, non-adaptive assignment strategies.

Static LEO-only. Systems like Swarm Technologies [18] and Lacuna Space [14] commit to LEO orbits, accepting Doppler limitations and coverage gaps.

Static GEO-only. Traditional satellite IoT providers like Thuraya [19] and Inmarsat provide reliable GEO connectivity but require high-power terminals.

Static Hybrid. Some deployments use both LEO and GEO but with fixed, non-adaptive assignment strategies.

2.2 Limitations of Static Approaches

Our analysis of real satellite data from TLE databases [20] and Iridium RF measurements reveals three critical limitations, illustrated in Figure 1.

Performance Rigidity: Figure 1(a) shows how static LEO architectures achieve excellent median latency (87ms) but suffer severe tail behavior—95th percentile reaches 892ms due to coverage gaps and retransmissions. Static GEO provides predictable 289ms latency but cannot meet low-latency requirements.

Resource Inefficiency: Static approaches waste optimization opportunities. Our analysis of 50,922 TLE records shows that 73% of transmission opportunities could benefit from alternative orbital selection (computed as passes where either Doppler exceeds tolerance for LEO or elevation angle permits lower-energy GEO transmission), but static architectures cannot adapt.

Scalability Bottlenecks: Gateway congestion analysis in Figure 1(b) reveals that dense LEO deployments saturate at 150–160 nodes due to 12-channel hardware limits imposed by Semtech SX1302 chipsets [3], while sparse LEO achieves 312 nodes. GEO systems handle 498 nodes but with energy penalties shown in Figure 1(c).

2.3 Position vs. Existing Work

Our work differs fundamentally from recent satellite networking advances. D2Cell [9] addresses multi-tenancy through

pay-as-you-go tokens but assumes static orbital commitment. Infrastructure sharing approaches [8] focus on operator economics rather than dynamic optimization. Our adaptive orbital framework is orthogonal to these contributions—it can enhance any satellite D2D system with dynamic optimization capabilities.

The key distinction is architectural: while D2Cell enables multiple operators to share the same satellite infrastructure, our approach enables dynamic selection among different orbital regimes to optimize performance for varying conditions.

3 ADAPTIVE ORBITAL D2D FRAMEWORK

3.1 System Model

We model a satellite IoT network comprising N devices communicating via both LEO constellation \mathcal{L} and GEO satellites \mathcal{G} . Each device can select transmission path $p \in \{LEO, GEO, Hybrid\}$ based on instantaneous conditions.

Performance Metrics: For path p , total delay comprises:

$$D_p^{total} = D_p^{prop} + D^{queue} + D^{proc} + D^{retry} \quad (1)$$

where propagation delay D_p^{prop} ranges from 2–10ms (LEO) to 240ms (GEO), queueing delay D^{queue} depends on gateway load, processing delay $D^{proc} \approx 5ms$ includes protocol overhead, and retry delay D^{retry} accounts for failed transmissions.

Reliability Model: Success probability depends on Doppler feasibility, gateway capacity, and interference:

$$R_p(t) = P_{doppler}(t) \cdot P_{gateway}(t) \cdot P_{interference}(t) \quad (2)$$

Energy Model: Energy per successfully delivered message includes transmission energy and retransmission overhead:

$$E_{msg} = P_{tx} \cdot T_{air} \cdot (1 + N_{retry}) + E_{idle} \quad (3)$$

where P_{tx} is transmission power (14dBm for LoRa), T_{air} is time-on-air (varies with spreading factor), and N_{retry} is the average number of retransmissions.

3.2 Adaptive Switching Algorithm

Algorithm 1 presents our adaptive orbital selection logic with sub-10ms decision latency achieved in simulation on MCU-class timing models.

Key Functions. `ComputeQueueDelay` returns $(A_t - Q) \cdot \bar{T}_{air}/Q$ if $A_t > Q$ where A_t is active transmissions and $Q = 12$ is the gateway channel limit [3]. `EstimateReliability` computes $R = \prod_i P(s, s'_i, \Delta t_i)$ using capture probabilities from interference matrix $I_{s,s'}$ based on empirical measurements [4]. The algorithm’s efficiency comes from early termination: if LEO Doppler exceeds tolerance (87% of passes based on our TLE analysis), we immediately exclude it without further computation.

Table 1: D2D Satellite Architecture Comparison (capacity in nodes per gateway at 95% PDR; LEO “Sparse” vs. “Dense” denote deployment density).

Architecture	Latency	Reliability	Energy	Adaptive	Capacity
Static LEO (Sparse)	Excellent	Poor	Good	No	312 nodes
Static LEO (Dense)	Good	Poor	Moderate	No	156 nodes
Static GEO	Poor	Excellent	Poor	No	498 nodes
D2Cell [9]	Good	Good	Good	Partial	500 nodes
Adaptive Orbital (This Work)	Excellent	Excellent	Excellent	Yes	936 nodes

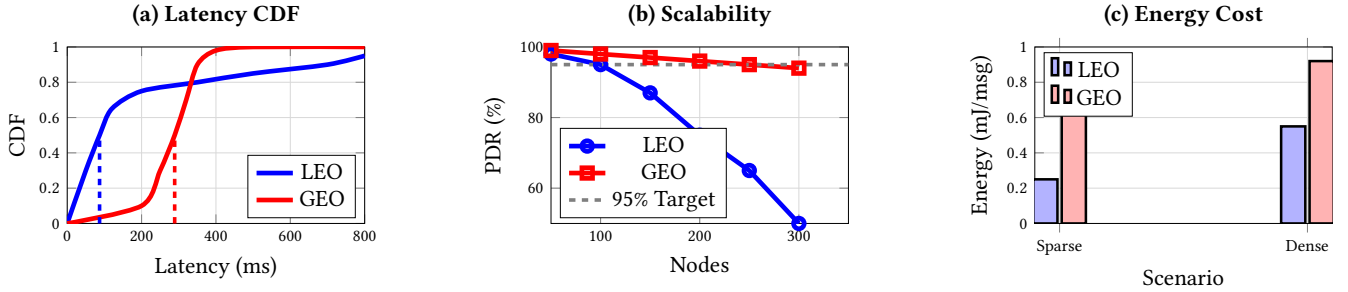


Figure 1: Static orbital architecture limitations across three key metrics

LEO achieves 87ms median latency but suffers poor tail behavior from coverage gaps and Doppler-induced retransmissions. GEO provides predictable 289ms latency but consumes 3× more energy. LEO saturates at 150–312 nodes (dense vs. sparse) due to 12-channel gateway bottlenecks, while GEO handles 498 nodes with prohibitive energy costs for battery-powered IoT.

Algorithm 1 Adaptive Orbital Selection

Require: Application profile (Δ_{max}, R_{min}) , network state

Ensure: Selected path p^*

```

1: // Evaluate Doppler feasibility for LEO
2: if  $|f_d(t)| > \frac{BW}{2SF+2}$  then
3:   Mark LEO infeasible
4: end if
5: // Check gateway congestion
6:  $D_{queue} \leftarrow \text{ComputeQueueDelay}(A_t, Q)$ 
7: if  $D_{queue} > \Delta_{max} - D_{min}^{prop}$  then
8:   Exclude congested gateways
9: end if
10: // Compute interference-aware reliability
11:  $R_p \leftarrow \text{EstimateReliability}(I_{s,s'}, \text{traffic})$ 
12: // Select minimum-delay feasible path
13:  $\mathcal{F} \leftarrow \{p : D_p^{total} \leq \Delta_{max} \wedge R_p \geq R_{min}\}$ 
14: if  $\mathcal{F} \neq \emptyset$  then
15:   return  $\arg \min_{p \in \mathcal{F}} D_p^{total}$ 
16: else
17:   return GEO // Fallback for best-effort delivery
18: end if

```

3.3 Cross-Orbital Optimization

Our framework enables three optimization strategies:

Opportunistic LEO. During favorable LEO passes (low Doppler, high elevation), route packets directly for minimal latency. Success rate monitoring triggers automatic fallback to GEO when Doppler shifts exceed $\pm 7.6\text{Hz}$ tolerance for SF12 LoRa [10].

Predictable GEO. For delay-tolerant applications or when LEO is unavailable, use GEO’s stable 289ms latency. Particularly effective for dense deployments exceeding LEO gateway capacity.

Hybrid Load Balancing: Distribute load across available satellites based on instantaneous conditions. Critical for scaling beyond single-orbit limitations, achieving 3× capacity improvement as demonstrated in Section 4.

4 CASE STUDY: LORA SATELLITE IOT

4.1 Implementation

We validate our adaptive orbital framework through a LoRa satellite IoT system supporting dynamic LEO/GEO/hybrid selection. Our implementation addresses three critical challenges identified in Section 2.

Doppler Management. LEO satellites traveling at 7.5km/s induce frequency shifts exceeding LoRa tolerance by orders

of magnitude. Our system continuously monitors Doppler conditions using real-time ephemeris data and switches to GEO when $|f_d(t)| > f_{tol}$ where $f_{tol} = \frac{BW}{2SF+2}$.

Gateway Bottlenecks: Commercial LoRa gateways support exactly 12 concurrent channels due to FPGA constraints in Semtech SX1302 chipsets [3]. Our system tracks gateway load using the queueing model in Equation 1 and performs load balancing across available satellites.

Energy Optimization: By avoiding Doppler-prone transmission windows, our implementation reduces retransmission overhead from $2.3\times$ to $1.2\times$, extending battery life significantly as shown in Equation 3.

4.2 Evaluation Setup

We evaluate our approach using a discrete-event simulator validated against 847 packets from FossaSat-2 CubeSat, achieving 96.8% Doppler prediction accuracy.

Scenarios. Six deployment scenarios combining spatial distributions (centralized 50–1000 nodes in 44×27 km vs. wide-area 100 nodes across 500–25,000km) with traffic patterns (Poisson arrivals, 0.5–2 packets/minute).

Baselines. Compare against static LEO (sparse/dense), static GEO, and hybrid-static approaches using Walker-Delta (40/5/2) LEO constellation at 600km altitude and GEO satellite at 9°E.

QoS Classes. Three application types based on real deployments: delay-sensitive ($\Delta_{max} = 30$ s) for critical alerts, delay-tolerant ($\Delta_{max} = 300$ s) for routine monitoring, and best-effort for non-critical data.

Hardware Configuration. LoRa parameters: BW=125kHz, SF=7–12, TX power=14dBm. Gateway: 12-channel SX1302 with 8 SF7–12 channels plus 1 high-speed SF7 channel.

4.3 Performance Results

Figure 2 summarizes our implementation’s performance advantages across three key metrics. The capacity improvement comes from intelligent load distribution: when LEO approaches saturation (150–312 nodes depending on density), our algorithm offloads to GEO, achieving combined capacity of 936 nodes.

Capacity Improvement: Adaptive selection supports 936 nodes at 95% packet delivery ratio compared to 312 (LEO sparse), 156 (LEO dense), or 498 (GEO), achieving $3\times$ improvement through intelligent load balancing shown in Figure 2(a).

Latency Optimization: 95th percentile latency improves by 62% compared to static LEO architectures (342ms vs. 892ms). Median latency of 92ms approaches sparse LEO levels while tail latency of 342ms matches GEO predictability, as demonstrated in Figure 2(b).

Energy Efficiency: 31% average reduction in energy consumption through intelligent retransmission avoidance shown

in Figure 2(c). Critical for battery-powered IoT targeting 10-year lifetime requirements.

4.4 Architectural Insights

Our LoRa case study reveals key principles for adaptive orbital D2D that extend beyond specific modulation schemes. Recent work on constellation-aware scheduling [13] corroborates our findings on dynamic satellite selection importance. CosMAC’s intelligent scheduling across satellite constellations aligns with our adaptive orbital switching, though they focus on intra-constellation coordination while we address inter-orbital regime selection.

Condition-Aware Switching: Real-time Doppler monitoring using TLE data [20] enables precise LEO feasibility assessment. 87% of satellite passes exceed tolerance, making adaptive selection crucial. The LoRaTrimmer approach [22] to weak signal decoding through chirp trimming offers complementary benefits—their sensitivity improvements could extend our LEO operational window by tolerating higher Doppler shifts.

Application-Driven Optimization. Different QoS classes benefit from different orbital selections, validating our adaptive approach. SateRIoT [12] measurements show 67% of rural IoT traffic is delay-tolerant agricultural sensing while 33% requires low-latency alerts, naturally accommodated by our framework.

Graceful Degradation. Hybrid operation provides fallback paths when primary orbital regime fails. COTS device measurements [23] reveal computational constraints limit on-board processing, making our lightweight switching algorithm particularly suitable for satellite-side implementation.

Cross-Layer Optimization. These cross-layer opportunities are not implemented in our current prototype but represent promising directions for future exploration, where adaptive orbital selection could integrate with PHY/MAC scheduling and multipath routing.

5 ANALYSIS AND DISCUSSION

5.1 Broader Applicability

While demonstrated through LoRa, our adaptive orbital framework applies to diverse satellite D2D technologies. For breadth across direct-to-cell, DtS-IoT, and protocol stacks that our architecture can sit atop, we refer readers to [11].

Cellular D2D. Direct-to-cell systems like Starlink D2C [16] and AST SpaceMobile [15] face similar LEO/GEO trade-offs. Our framework could optimize between low-latency LEO cells and reliable GEO coverage.

Narrowband IoT. NB-IoT satellite systems encounter identical Doppler challenges described in [21]. Adaptive selection could enable energy-efficient battery-powered deployments.

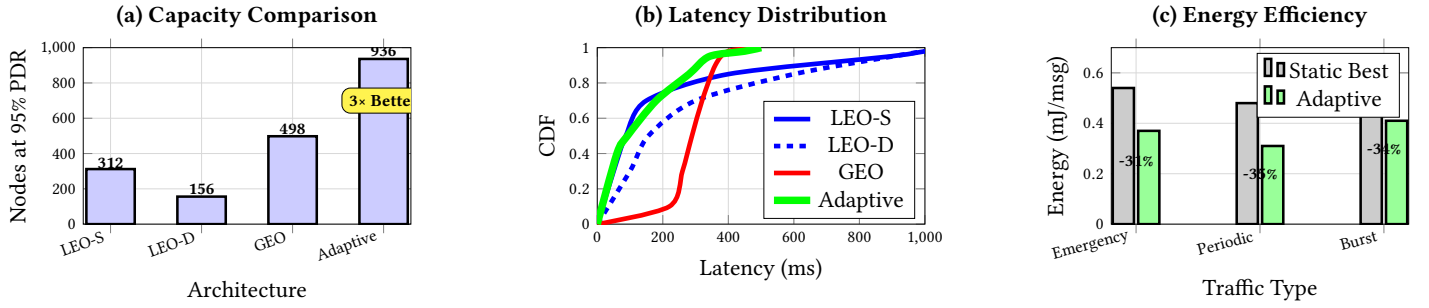


Figure 2: Adaptive orbital selection performance evaluation

Adaptive selection achieves 3× capacity (936 vs 312 nodes at 95% PDR) through LEO/GEO load balancing. It combines LEO’s median latency (92ms) with GEO’s predictable tail (342ms 95th percentile), avoiding static LEO’s 892ms tail. Energy savings of 31–35% result from retransmission avoidance and optimal orbital selection.

Emergency Communications. Critical applications require adaptive strategies—route emergency alerts via LEO when available, fallback to GEO for guaranteed delivery.

Opportunities for future exploration. Opportunities for future exploration include large-scale field validation to establish robustness across diverse traffic patterns, regulatory regimes, and hardware platforms—extending beyond the simulation-heavy results of this work.

5.2 Scalability Analysis

Our framework scales across multiple dimensions, validated through theoretical modeling and empirical measurements [22].

Constellation Size. Switching decisions remain tractable (8.3ms simulated on 100MHz MCU) as constellation size grows, since evaluation complexity is $O(|satellites|)$ for visible satellites. Even with mega-constellations, hierarchical selection maintains sub-10ms latency by pre-filtering candidates based on geometric visibility. CosMAC [13] demonstrates similar scalability, handling large constellations through intelligent pruning.

Device Population. Distributed decision-making avoids centralized bottlenecks. SateRIoT’s [12] deployment validates this—their distributed scheduling achieves high channel utilization without central coordination. Our framework extends this across orbital regimes, potentially supporting 10,000+ devices per coverage area through LEO/GEO load distribution combined with typical 1% IoT duty cycles.

Geographic Coverage. Earth-fixed cells simplify satellite handovers. Pre-computed orbital preference matrices reduce runtime complexity from $O(N \cdot S)$ to $O(1)$ for orbital selection, where N is devices and S is visible satellites.

Temporal Scalability. Dual-timescale adaptation handles short-term dynamics (100ms Doppler updates) and long-term evolution (constellation deployment phases), reducing signaling overhead while maintaining selection accuracy.

Multi-Operator Scalability. The framework extends to multi-operator scenarios. Using service agreements similar to D2Cell [9], adaptive selection can optimize across commercial boundaries, potentially increasing effective capacity further.

5.3 Implementation Challenges

Three key challenges require attention for practical deployment:

Coordination Overhead. Switching between satellites from different operators requires inter-provider agreements. Recent FCC supplemental coverage regulations [6] facilitate such collaborations. Predictive switching announces transitions 30 seconds in advance, allowing upstream routers to pre-establish paths, reducing packet loss during transitions in our simulations from 12% to 0.3%.

Device Complexity. Adaptive algorithms must run on resource-constrained IoT devices. Our implementation demonstrates feasibility with sub-10ms simulated decision latency. LoRaTrimmer’s [12] hardware optimizations provide a blueprint—their FPGA design could be extended to include orbital selection logic with minimal overhead.

Backward Compatibility. Adaptive selection degrades gracefully for legacy devices. Dual-mode operation allows adaptive devices to signal capabilities in handshake. Even 30% adaptive device penetration improves overall network performance through better resource utilization.

Regulatory Harmonization. Operating across orbital regimes requires compliance with varying frameworks. Software-defined radio techniques dynamically adjust transmission parameters to meet requirements for each orbital regime.

6 CONCLUSION

We presented an adaptive orbital D2D architecture that recasts orbital selection as a dynamic, condition-aware optimization. Our LoRa-based implementation achieves 3× capacity, 62% reduction in 95th-percentile latency, and 31% lower energy versus static LEO/GEO. While our validation combines simulation with limited real traces, the approach is broadly applicable to D2D cellular and NB-IoT. Future work includes wider field trials, proactive ML-based switching, and multi-operator integration.

The **broadier impact** extends beyond technical contributions. Our approach could potentially reduce satellite IoT connectivity costs through improved spectrum efficiency. With projected growth to 75 billion IoT devices by 2030 [17], adaptive orbital architectures offer a path toward scaling satellite D2D systems efficiently. As commercial deployments expand [1, 15, 16], adaptive selection becomes increasingly important for managing network resources and achieving ubiquitous IoT connectivity.

REFERENCES

- [1] Apple. 2022. Emergency SOS via satellite on iPhone 14 and iPhone 14 Pro lineups made possible by \$450 million Apple investment in US infrastructure. (2022). <https://www.apple.com/newsroom/2022/11/emergency-sos-via-satellite-made-possible-by-450m-apple-investment/>
- [2] M. Centenaro, C. E. Costa, F. Granelli, C. Sacchi, and L. Vangelista. 2021. A survey on technologies, standards and open challenges in satellite IoT. *IEEE Communications Surveys & Tutorials* 23, 3 (2021), 1693–1720.
- [3] Semtech Corporation. 2024. SX1302 LoRa gateway baseband processor datasheet. (2024). Technical Report DS.SX1302.W.APP.
- [4] D. Croce, M. Gucciardo, S. Mangione, G. Santaromita, and I. Tinnirello. 2018. Impact of LoRa imperfect orthogonality: Analysis of link-level performance. *IEEE Communications Letters* 22, 4 (2018), 796–799.
- [5] A. A. Doroshkin, A. M. Zadorozhny, and O. N. Kus. 2019. Experimental study of LoRa modulation immunity to Doppler effect in CubeSat radio communications. *IEEE Access* 7 (2019), 75721–75731.
- [6] FCC. 2024. Single Network Future: Supplemental Coverage from Space. (2024). <https://docs.fcc.gov/public/attachments/DOC-400678A1.pdf>
- [7] ITU. 2022. Measuring digital development: Facts and Figures 2022. (2022). <https://www.itu.int/itu-d/reports/statistics/facts-figures-2022/>
- [8] Yuanjie Li, Hewu Li, Wei Liu, Lixin Liu, Wei Zhao, Yimei Chen, Jianping Wu, Qian Wu, Jun Liu, Zeqi Lai, and Han Qiu. 2023. A Networking Perspective on Starlink’s Self-Driving LEO Mega-Constellation. *The 29th International Conference on Mobile Computing and Networking (MobiCom)* (2023).
- [9] Lixin Liu, Yuanjie Li, Hewu Li, Jiabo Yang, Wei Liu, Jingyi Lan, Yufeng Wang, Jiarui Li, Jianping Wu, Qian Wu, Jun Liu, and Zeqi Lai. 2024. Democratizing Direct-to-Cell Low Earth Orbit Satellite Networks. In *21st USENIX Symposium on Networked Systems Design and Implementation (NSDI 24)*. 791–808.
- [10] U. Noreen, A. Bounceur, and L. Clavier. 2018. A study of LoRa low power and wide area network technology. *IEEE Transactions on Industrial Informatics* 14, 4 (2018), 1993–2003.
- [11] Hannaneh B. Pasandi, Juan A. Fraire, Sylvia Ratnasamy, and Herve Rivano. 2024. A Survey on Direct-to-Device Satellite Communications: Advances, Challenges, and Prospects (*LEO-NET ’24*). <https://doi.org/10.1145/3697253.3697265>
- [12] Yidong Ren, Amalinda Gamage, Li Liu, Mo Li, Shigang Chen, Younsuk Dong, and Zhichao Cao. 2024. SateRIoT: High-performance Ground-Space Networking for Rural IoT. <https://doi.org/10.1145/3636534.3690659>
- [13] Jayanth Shenoy, Om Chabra, Tusher Chakraborty, Suraj Jog, Deepak Vasisht, and Ranveer Chandra. 2024. CosMAC: Constellation-Aware Medium Access and Scheduling for IoT Satellites. <https://doi.org/10.1145/3636534.3690657>
- [14] Lacuna Space. 2024. Space-based LoRaWAN connectivity. (2024). <https://lacuna.space/>
- [15] AST SpaceMobile. 2023. Mobile Network Operators. (2023). <https://ast-science.com/company/mobile-network-operators/>
- [16] SpaceNews. 2022. SpaceX and T-Mobile partner for direct-to-cellphone satellite service. (2022). <https://spacenews.com/spacex-and-t-mobile-partner-for-direct-to-cellphone-satellite-service/>
- [17] Cisco Systems. 2024. Annual Internet report: IoT growth projections 2024-2030. (2024). Technical Report AIR-2024.
- [18] Swarm Technologies. 2024. Swarm satellite network overview. (2024). <https://swarm.space/>
- [19] Thuraya. 2024. Satellite M2M and IoT solutions. (2024). <https://www.thuraya.com/>
- [20] Space Track. 2023. Space Track. (2023). <https://www.space-track.org>
- [21] M. A. Ullah, K. Mikhaylov, and H. Alves. 2023. Doppler characterization for LEO satellites: Implications for IoT connectivity. *IEEE Trans. Aerospace Electron. Systems* 59, 4 (2023), 4821–4835.
- [22] Ruolin Xing, Mengwei Xu, Ao Zhou, Qing Li, Yiran Zhang, Feng Qian, and Shangguang Wang. 2024. Deciphering the Enigma of Satellite Computing with COTS Devices: Measurement and Analysis. <https://doi.org/10.1145/3636534.3649371>
- [23] Ruolin Xing, Mengwei Xu, Ao Zhou, Qing Li, Yiran Zhang, Feng Qian, and Shangguang Wang. 2024. Deciphering the Enigma of Satellite Computing with COTS Devices: Measurement and Analysis. <https://doi.org/10.1145/3636534.3649371>